Transgenic Mice Overexpressing Neuropeptide Y in Noradrenergic Neurons

A Novel Model of Increased Adiposity and Impaired Glucose Tolerance

Suvi T. Ruohonen,[1,2] Ullamari Pesonen,[1] Niko Moritz,[3] Katja Kaipio,[1,2] Matias Röyttä,[4] Markku Koulu,[1] and Eriika Savontaus[1,5]

OBJECTIVE—A functional polymorphism leucine 7 proline in the human *neuropeptide Y* (*NPY*) gene leading to increased NPY release from sympathetic nerves is associated with traits of metabolic syndrome. Although hypothalamic NPY neurons play an established role in promoting positive energy balance, the role of NPY colocalized with norepinephrine in sympathetic nervous system and brain noradrenergic neurons remains obscure.

RESEARCH DESIGN AND METHODS—To clarify the role of NPY in noradrenergic neurons, we generated a transgenic mouse overexpressing NPY under dopamine–β-hydroxylase promoter and characterized the metabolic phenotype of the OE-NPY$^{D\beta H}$ mouse.

RESULTS—NPY levels are increased by 1.3-fold in adrenal glands and 1.8-fold in the brainstem but not in the hypothalamus in OE-NPY$^{D\beta H}$ mice. They display increased white adipose tissue mass and cellularity and liver triglyceride accumulation without hyperphagia or increased body weight. Hyperinsulinemia and impaired glucose tolerance develop by the age of 6 months in the OE-NPY$^{D\beta H}$ mice. Furthermore, circulating ghrelin is significantly increased in comparison with wild-type mice.

CONCLUSIONS—The present study shows that even a moderate increase in NPY levels in noradrenergic neurons leads to disturbances in glucose and lipid metabolism. The OE-NPY$^{D\beta H}$ mouse is an interesting new model to investigate the pathophysiology of some key components of the cluster of abnormalities characterizing the metabolic syndrome. ***Diabetes*** **57:1517–1525, 2008**

From the [1]Department of Pharmacology, Drug Development and Therapeutics, University of Turku, Turku, Finland; the [2]Drug Discovery Graduate School, University of Turku, Turku, Finland; the [3]Department of Orthopedics and Traumatology, University of Turku, Turku, Finland; the [4]Department of Pathology, University of Turku, Turku, Finland; and [5]Clinical Pharmacology, TYKSLAB, Health Care District of Southwest Finland, Turku, Finland.

Corresponding author: Dr. Eriika Savontaus, Department of Pharmacology, Drug Development and Therapeutics, University of Turku, FI-20014 Turun yliopisto, Finland. E-mail: eriika.savontaus@utu.fi.

Received for publication 28 May 2007 and accepted in revised form 31 January 2008.

Published ahead of print at http://diabetes.diabetesjournals.org on 14 February 2008. DOI: 10.2337/db07-0722.

AUC, area under the curve; BMD, bone mineral density; DβH, dopamine–β-hydroxylase; H-E, hematoxylin-eosin; IGTT, intraperitoneal glucose tolerance test; IRES, internal ribosomal entry site; NE, norepinephrine; NPY, neuropeptide Y; RIA, radioimmunoassay; SNS, sympathetic nervous system; WAT, white adipose tissue.

Neuropeptide Y (NPY) plays a well-established role in the hypothalamic control of body energy balance. It is one of the key components of the interconnected orexigenic network, which is upregulated in states of negative energy balance. NPY is a very potent orexigenic peptide, and when chronically administered into the central nervous system, it leads to increased food intake, weight gain, and adiposity (1–3). NPY-induced obesity is not only due to hyperphagia; centrally administered NPY also promotes white adipose tissue (WAT) lipid storage, inhibits brown adipose tissue thermogenesis, and induces hyperinsulinemia and hypercorticosteronemia (4–6). Increased hypothalamic NPY is also an essential feature of leptin-deficient obesity, which is attenuated by genetic depletion of NPY (7). Although there is plenty of evidence on the key role of NPY in the regulation of energy balance in rodents, the evidence is scarce in humans and based mainly on the functional leucine 7 proline (L7P) polymorphism of the preproNPY associated with alterations in glucose and lipid metabolism and development of atherosclerosis (8).

In addition to the NPY neurons of the hypothalamus, NPY is widely distributed in the central and peripheral nervous system. In the periphery, NPY is co-stored and co-released in postganglionic sympathetic neurons and chromaffin cells of adrenal medulla with norepinephrine (NE) (9,10). In the brain, NPY is also colocalized with NE in noradrenergic neurons in the medulla and the brainstem (11). The role of the extrahypothalamic NPY in regulation of energy homeostasis has not gained much attention, although NPY and its receptors are located in key peripheral tissues, such as adipose tissue, liver, and pancreas.

To address the role of NPY colocalized with NE in sympathetic nervous system (SNS) and brain noradrenergic neurons, we generated a transgenic mouse model overexpressing NPY in the peripheral SNS and in the noradrenergic system of the brain. The overexpression was targeted at adrenergic and noradrenergic neurons with promoter of the *dopamine–β-hydroxylase* (*DβH*) gene (12). NPY level in the hypothalamus is left unaltered, which facilitates studying the extrahypothalamic effects of NPY. In this study, we show that moderate overexpression of NPY in the SNS and brain noradrenergic nuclei leads to significant impairment of lipid and glucose metabolism in the DβH-NPY transgenic mice.

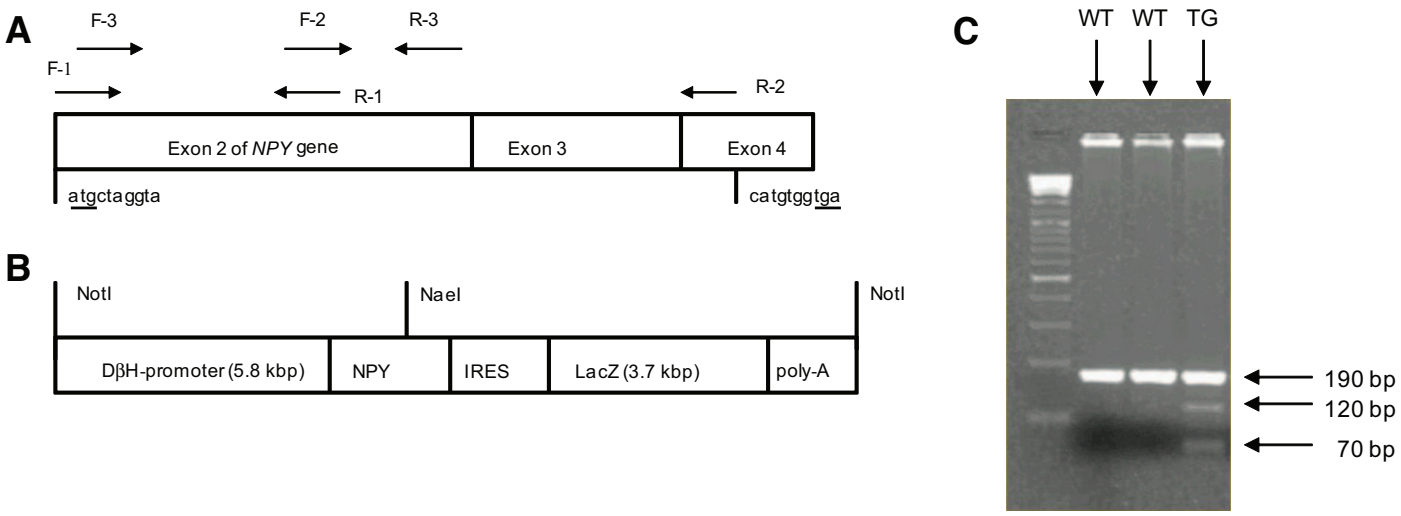

FIG. 1. The PCR primers and the transgene construction. *A*: A schematic drawing of the NPY cDNA and the locations of the three primer pairs used in the study. The genetic start codon (atg) and the stop codon (tga) are also depicted. The sequences for forward (F) and reverse (R) primers can be found in the text (RESEARCH DESIGN AND METHODS). *B*: A depiction of the DβH-NPY transgene construct containing the DβH-promoter, NPY cDNA, IRES sequence, *LacZ* gene, and the poly-A tail. In the PCR, a silent mutation (*Nae*I restriction site) was created 120 bp starting from exon 2 to distinguish the transgenic and the endogenous NPY. The genes are not proportionally correct. poly-A, polyadenylase tail. *C*: PCR products digested with *Nae*I from mouse genomic DNA. *Left lane*, a 100-bp ladder. WT, wild type; TG, transgenic.

RESEARCH DESIGN AND METHODS

DβH-NPY-IRES-LacZ transgene construct and generation of transgenic mice. Total RNA from a mouse hypothalamus was purified by the GenElute Mammalian Total RNA kit (Sigma Diagnostics, St. Louis, MO) and synthesized into cDNA (M-MLV RT RNase kit; Promega, Madison WI). To isolate the 300-bp *preproNPY* coding cDNA, exons 2 and 3 and part of exon 4 were amplified by PCR using two primer pairs: forward-1, 5′-CATGTTATGCATAT GCTAGGTAACAAGCGA-3′, with reverse-1, 5′-TCCTCTGCCGGCGCGTC-3, and forward-2, 5′-GACGCGCCGGCAGAGGA-3′, with reverse-2, 5′-CAAGTA ATGCATTCACCACATGGAAGGGTC-3′ (Fig. 1*A*). In the third PCR run, exons were joined by using the primers forward-1 and reverse-2. A plasmid containing a viral 580-bp internal ribosomal entry site (IRES) followed by a 3.7-kb reporter gene *LacZ* encoding β-galactosidase was linearized, and the *preproNPY* cDNA was ligated upstream of the IRES fragment. IRES enables cap-independent translation of *preproNPY* and *LacZ* into single transgenic mRNA, which results in coexpression of both genes from the same promoter (13). The bicistronic NPY-IRES-LacZ construct was inserted downstream of the previously described 5.8-kb promoter of the human *DβH* gene (12), and the final 10.6-kb transgene construct was excised from the vector with *Not*I (Fig. 1*B*). Thus, DβH promoter drives the expression of transgenic NPY and LacZ, and positive β-galactosidase staining can be used as a marker of transgene expression. The construct was sequenced gene by gene to verify the correct alignment of base pairs before it was microinjected into fertilized FVB/n eggs. The oocytes were transferred into pseudopregnant FVB/n females to generate hemizygous offspring.

Genotyping of mice. Genomic DNA was isolated from tail biopsies from weaned pups with a commercial kit (Gentra, Minneapolis, MN). Genotypes were determined by PCR using forward-3 primer 5′-AACAAACGAAT GGGGCTGTGT-3′ and reverse-3 primer 5′-GTGATGAGATTGATGTAGT GTCG-3′ located in exon 2 of the *preproNPY* gene (Fig. 1*A*). The PCR products were digested with *Nae*I. Wild-type DNA showed a single 190-bp band and transgenic DNA 190-, 120-, and 70-bp bands (Fig. 1*C*). Eight transgene DNA-positive founder mice (F1) were produced and bred with FVB/n mice to produce F2 hemizygous transgenic animals. β-Galactosidase expression showed most consistent staining in line number 32, which was chosen for further studies and backcrossed to C57BL/6 for six generations.

Mouse experiments. Groups (n = 7–15) of 3- and 6-month-old male and 6-month-old female mice (C57BL/6) were used unless stated otherwise. The mice were kept in an animal room maintained at 21 ± 1°C with a fixed 12-h light/12-h dark cycle. Standard rodent chow (SDS, Essex, U.K.) and water were available ad libitum. Wild-type littermates were used as control mice. We obtained terminal blood samples from vena cava (plasma) or trunk blood (serum) after a 4-h fast between 1000 and 1400 h to analyze levels of NPY, leptin, resistin, corticosterone, ghrelin, and triglyceride. All samples were stored at −70°C and treated in duplicate. To access vena cava, the mice were quickly anesthetized with ketamine (Ketalar 75 mg/kg i.p.) and medetomidine (Domitor 1 mg/kg i.p.). Otherwise, mice were killed by decapitation. Samples for glucose and insulin analyses were obtained from tail vein after a 4-h fast. Experimental procedures were approved by the local animal ethics committee (The Lab-Animal Care and Use Committee at the University of Turku).

Bacterial β-galactosidase expression. Coronary brain (80-μm) and adrenal (35-μm) frozen sections were mounted on gelatin-coated slides and stained for *Escherichia coli* β-galactosidase as previously described (14).

NPY immunohistochemistry. Brains and adrenal glands were immersed in a 4% paraformaldehyde fixative overnight and cryoprotected with 30% sucrose overnight before freezing. Frozen sections of coronary brain and adrenal glands (35 μm thick) were cut with a cryostat and placed in PBS with 0.01% Triton-X. Free-floating sections were washed in PBS and preincubated with blocking buffer (5% goat normal serum and 0.01% Triton-X in PBS) for 30 min at room temperature. The sections were incubated overnight at 4°C with rabbit polyclonal anti-NPY antibody (Affiniti Research Products, Exeter, U.K.) diluted 1:1,500 followed by incubation biotinylated goat anti-rabbit antibody (1:3,000) (Molecular Probes, Eugene, OR) for 1 h at room temperature. A Standard Vectastain Elite ABC kit (Vector Laboratories, Burlingame, CA) was used in conjunction with the biotinylated antibody, and subsequent horseradish peroxidase activity was developed using 3,3′-diaminobenzidene as a substrate (Sigma Fast DAB tablets; Sigma Diagnostics). The immunostaining was visualized using light microscopy.

NPY protein concentrations in tissues and plasma. Blood was collected from 3-month-old male and female mice (n = 8/group). The brain and both adrenal glands were removed and washed with cold saline. Medial basal hypothalamus was isolated with a mouse brain block using a 2-mm section caudal to the optic nerve chiasma, excluding hippocampal and cortical areas. The brainstem section extended 3 mm caudal from the hypothalamic section, including locus coeruleus and A5 noradrenergic nuclei, but the cerebellum and cerebral cortex were discarded. In adrenal glands, the majority of NPY is localized within the medulla (15). Therefore, whole adrenal glands were used in this study. Tissues were homogenized with 500 μl 0.1 N HCl and placed immediately on ice. The tissue homogenates were sonicated, and NPY concentrations were determined with a EURIA-NPY radioimmunoassay (RIA) kit (Euro-Diagnostica, Malmö, Sweden) with some modifications to the instructions for the kit: Tissues were diluted to 0.1 mol/l Na_2HPO_4, buffer pH 8.3, and the standard curve standards in the manufacturer's diluent. NPY concentrations were adjusted to the tissue protein levels determined with a BCA Protein Assay Reagent kit (Pierce Biotechnology, Milwaukee, WI) using phosphate buffer as a diluent. Plasma NPY concentrations were determined with the RIA kit by diluting plasma 1:4 to the assay buffer with 5% BSA.

Body weights and food consumption. All mice used in the studies were weighed before killing the animals. Additionally, a set of adult males and females were separated into single cages and allowed to adjust to the change for 1 week. The mice were weighed weekly for 3–8 weeks. Food was freely available but carefully weighed every 2 days to calculate the average consumption and spillage of chow per day per mouse.

Spontaneous locomotor activity test. Five-month-old male mice (n = 8–11/group) were placed individually into transparent polypropylene locomotor activity cages housed in a photo-beam recording system (San Diego

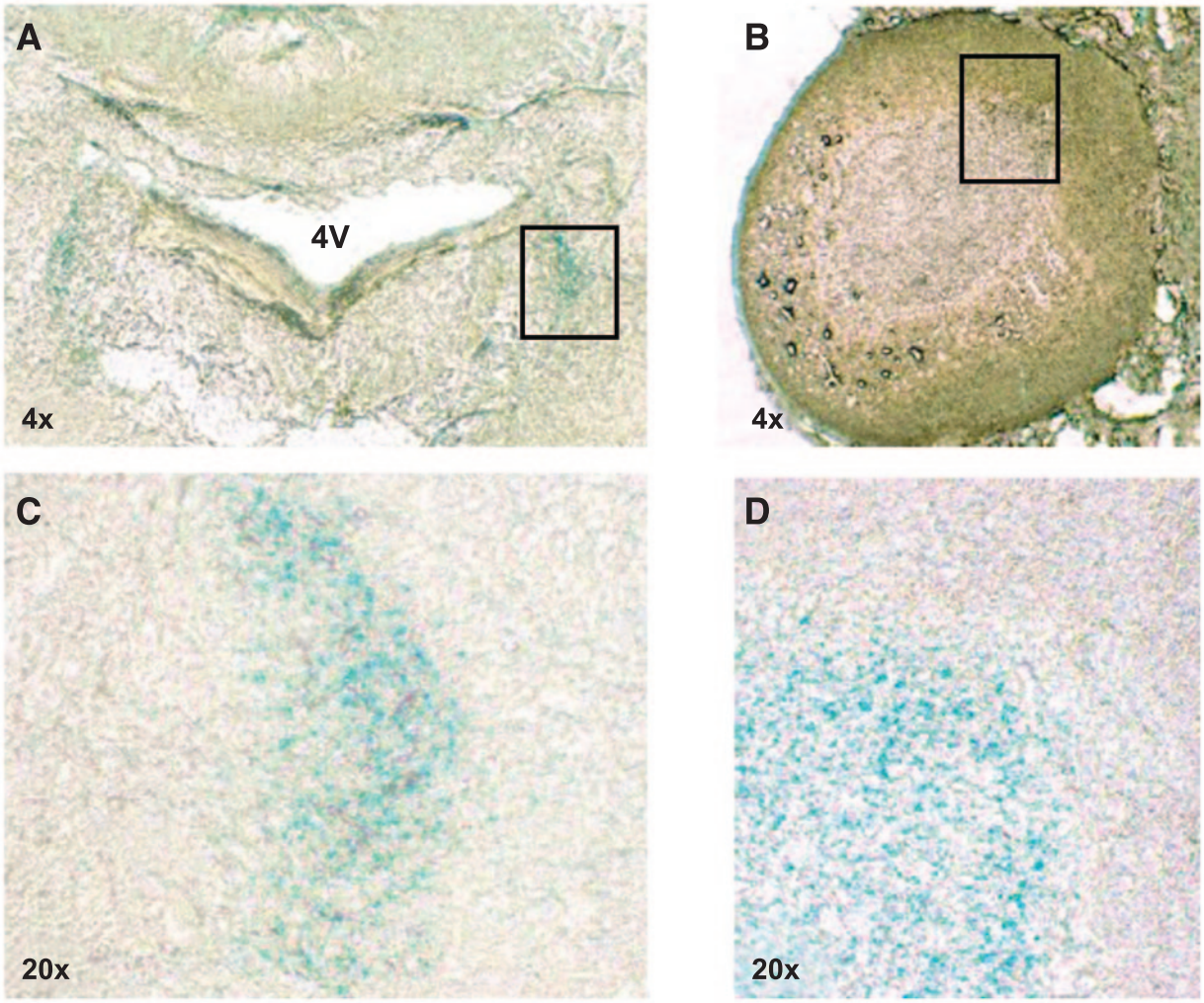

FIG. 2. Expression of *DβH-LacZ* transgene in the brainstem and adrenal glands. *A*: Section through a transgenic brainstem stained for *E. coli* β-galactosidase viewed with a light microscope. Locus coeruleus nuclei around the 4th ventricle (4V) show positive staining as seen in ×20 magnification (*C*). *B*: Section through a transgenic adrenal gland stained and viewed for β-galactosidase as in *A*. The medulla shows transgene expression, whereas the cortex does not, as seen in ×20 magnification (*D*).

Instruments, San Diego, CA). The locomotor activity was measured over 10-min intervals for 24 h. The measurements started at 1200 h after 24-h habituation.

Core body temperature. Rectal body temperatures were measured with a digital thermometer (Ellab, Roedovre, Denmark) from 3-month-old male and female mice (n = 7–10/group) between 1000 and 1200 h.

Bone mineral density. The nose-anal lengths and femur lengths of the 3-month-old male mice (n = 6/group) were measured. Femurs were imaged with a Skyscan 1072 Micro-CT (Skyscan, Aartselaar, Belgium). The Micro-CT system was calibrated with two hydroxyapatite phantoms with known densities of 250 and 750 mg/cm^3. For each specimen, a volume of interest containing trabecular bone and bone marrow was manually defined, and the trabecular bone was separated from the bone marrow using a global thresholding technique.

Body fat weight and fat cell size. WAT weight was determined by collecting the subcutaneous, epididymal/gonadal, and retroperitoneal fat pads at death. The fat cell sizes were determined from a total of eight gonadal fat pads from 3-month-old female mice as previously described (16). Cells were analyzed and imaged under a light microscope, and diameters were calculated using Cell*A imaging software (Soft Imaging System, Münster, Germany).

Hepatic and circulating lipids. Liver lipid contents were isolated and purified with the Folch method (17). Plasma, serum, and tissue triglycerides were quantified with Free Glycerol Reagent (F6428) and Triglyceride Reagent (T2449; Sigma Diagnostics). Serum total cholesterol from 6-month-old females was measured with the BioVision Cholesterol Quantitation kit (BioVision, Mountain View, CA).

Insulin, corticosterone, adipokine, and ghrelin assays. Circulating concentrations of insulin (ELISA kit; Mercodia, Uppsala, Sweden), corticosterone (RIA kit; MP Biomedicals, Orangeburg, NY), ghrelin (RIA kit; Linco Research, St. Charles, MO), leptin, and resistin (LINCO*plex* Adipokines kit; Linco Research) were measured using commercial kits.

Liver and skeletal muscle morphology and enzyme histochemistry. The left lateral lobes and gastrocnemius from male mice were dissected, placed in liquid nitrogen, and stored at −70°C. Frozen sections (5 μm) were cut and, based on the results from a pilot study, stained for hematoxylin-eosin (H-E), oil red O, and sudan black (liver) or for H-E and ATP 3.4 (muscle).

Intraperitoneal glucose tolerance test. Mice were fasted from 600 to 1000 h and administered intraperitoneally with glucose (5% [wt/vol], 1 g/kg body wt). Tail vein blood glucose was measured at 0, 20, 40, 60, and 90 min with the Precision Xtra Glucose Monitoring Device (Abbott Diabetes Care, Abbott Park, IL). Areas under the resultant glucose curves were calculated with the trapezoidal method in GraphPad Prism 4.3 software (GraphPad Software, San Diego, CA).

Statistical analyses. The results were compared with unpaired Student's t test between the genotypes. Logarithmic transformations were used if data were not normally distributed (D'Agostino and Pearson omnibus normality test). The nonparametric Mann-Whitney test was used if the distribution remained skewed after the transformation. Comparisons between the two genotypes and both sexes were analyzed with two-way ANOVA with Bonferroni post hoc test. Intraperitoneal glucose tolerance test (IGTT) and locomotor activity data were analyzed with repeated-measures two-way ANOVA. Correlation analyses were performed using linear regression to compare body weight or WAT weight with other variables (area under the curve [AUC] in IGTT, fasting insulin, and leptin) and glucose (AUC) with ghrelin. Statistical analyses were carried out using GraphPad Prism 4.3. Data are presented as

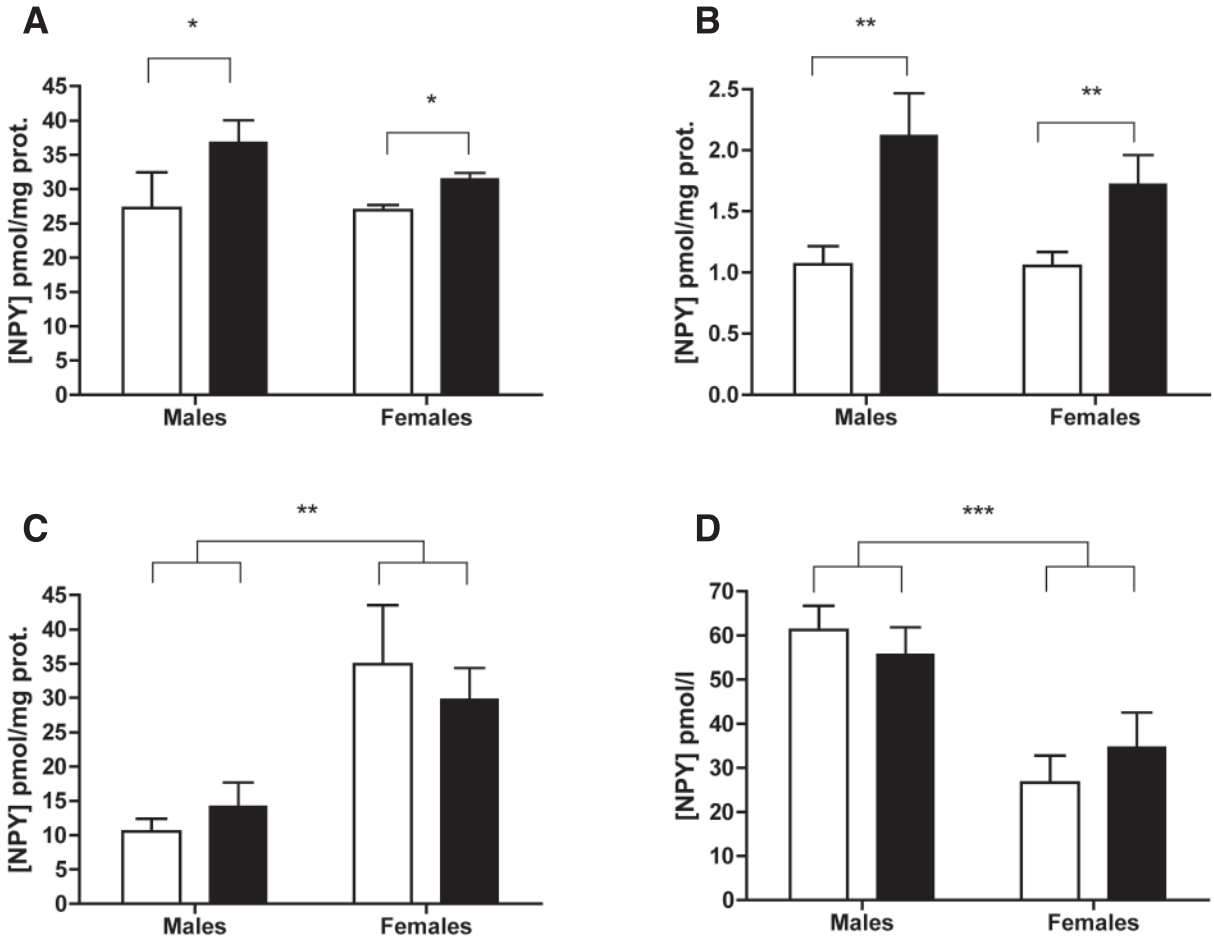

FIG. 3. Tissue and plasma NPY levels. NPY concentrations in adrenal glands (*A*), brain stem (*B*), hypothalamus (*C*), and plasma (*D*) of wild-type and OE-NPY$^{D\beta H}$ male and female mice (n = 8/group). Values are expressed as means ± SEM. □, wild-type mice; ■, OE-NPY$^{D\beta H}$ mice. *$P < 0.05$, **$P < 0.01$, and ***$P < 0.001$ by two-way ANOVA.

means ± SEM, and the results were considered statistically significant at $P < 0.05$.

RESULTS

Generation of DβH-NPY-IRES-LacZ transgenic mice. NPY- and LacZ-overexpressing mice under DβH promoter were generated, resulting in eight founders from which a line of transgenic mice was established. Genotype distributions matched expected Mendelian ratios. NPY overexpression does not result in embryonic lethality, and the mice produce pups normally. Transgene expression was visualized with β-galactosidase analysis, which showed strong and specific LacZ staining in adrenal medulla and the locus coeruleus and A5 nuclei of the brainstem (Fig. 2), which are areas known to contain dense noradrenergic innervation. Staining was faint in the hypothalamus, the cortex, the medial habenular nuclei, and the paraventricular thalamic nucleus. Blue color was observed only in the OE-NPY$^{D\beta H}$ mice, and no ectopic staining was observed in any of the sections. Examination of coronal brain sections and adrenal glands using immunohistochemistry with a specific NPY antibody revealed that in the OE-NPY$^{D\beta H}$ mice, NPY was detected in the same areas as those observed in wild-type littermates. These areas included adrenal medulla, the arcuate, the ventro-/dorsomedial and the periventricular nuclei of the hypothalamus, the lateral hypothalamic area, the hippocampus, the amygdala, the thalamus, and the locus coeruleus and A5 neurons of the brainstem. No site of ectopic NPY expression was observed in transgenic animals (data not shown).

Tissue and plasma NPY levels. The NPY concentrations in adrenal, brainstem, and hypothalamus homogenates and plasma were measured with RIA. The OE-NPY$^{D\beta H}$ mice had a significantly higher NPY concentration in the adrenals and in the brainstem compared with wild-type mice (genotype, $P < 0.05$ and 0.01, respectively; sex, NS; genotype × sex interaction, NS; Fig. 3*A* and *B*). NPY concentration in the hypothalamus did not differ between the genotypes but was increased in females in comparison with males (genotype, NS; sex, $P < 0.01$; genotype × sex interaction, NS; Fig. 3*C*). NPY concentration in plasma did not differ between the genotypes. However, NPY levels were significantly higher in male than in female mice (genotype, NS; sex, $P < 0.001$; genotype × sex interaction, NS; Fig. 3*D*).

Body weight, length, bone mineral density, and food intake. Body weights were recorded from mice at 3 and 6 months of age, and no difference between the genotypes was observed (Fig. 4*A*). During a weekly follow-up, the mice retained the body weights steadily, and no difference in the amount of food consumed between the wild-type and transgenic mice was observed (males, 4.12 ± 0.27 and 4.19 ± 0.30 g/day; females, 3.59 ± 0.53 and 3.64 ± 0.48 g/day, respectively; NS). The mice displayed similar body

and femur lengths at 3 months (wild type, 9.51 ± 0.14 and 1.46 ± 0.04 cm; OE-NPY$^{D\beta H}$, 9.48 ± 0.15 and 1.46 ± 0.04 cm, respectively; NS). Bone mineral density (BMD) did not differ between the genotypes (wild type, 1,119 ± 13.7; OE-NPY$^{D\beta H}$, 1,105 ± 27.5 mg/cm^3; NS).

Body adiposity. The OE-NPY$^{D\beta H}$ mice had significantly more WAT relative to controls at 3 and 6 months of age (Figs. 4*B* and *C* and 5*A*). Mean fat cell diameter was significantly smaller in the OE-NPY$^{D\beta H}$ fat pads (Fig. 5*B*). The triglyceride content of the OE-NPY$^{D\beta H}$ livers was increased already at 3 months (Table 1), but the livers were not enlarged and did not show severe fatty liver morphology. No differences in circulating triglyceride and cholesterol levels were observed (Table 1). Basic morphology of the skeletal muscle was similar between the genotypes (data not shown).

Spontaneous locomotor activity and body temperature. No differences in overall activity or number of rearings between the genotypes were observed (Fig. 6). Also, no difference in rectal body temperature between wild-type and OE-NPY$^{D\beta H}$ mice was observed (males, 37.16 ± 0.29 vs. 37.07 ± 0.46°C; females, 37.47 ± 0.31 vs. 36.84 ± 0.23°C, respectively; NS).

Endocrinological parameters. Six-month-old males had increased plasma insulin in comparison with wild-type males (Table 1), and the insulin values correlated positively with body weights in both genotypes (wild type, r = 0.60, $P < 0.05$; OE-NPY$^{D\beta H}$, r = 0.86, $P < 0.001$). Insulin levels of 3-month-old mice remained under the detection level of the insulin kit in both genotypes (Table 1). Leptin levels did not differ between the genotypes, although a tendency to increased leptin was seen in 6-month-old males (Table 1). There was no difference in corticosterone or resistin levels between the genotypes (Table 1). Ghrelin levels were significantly increased in the OE-NPY$^{D\beta H}$ mice over wild-type values (Table 1). In females, we did not observe any differences between the genotypes in plasma insulin, leptin, resistin, or corticosterone levels (data not shown).

IGTT. At 3 months, the glucose tolerance was normal in males and females. Six-month-old male OE-NPY$^{D\beta H}$ mice showed impaired glucose tolerance, although fasting glucose remained normal (Fig. 7). In mutant mice, the AUC in IGTT was significantly elevated compared with that in wild-type mice (Fig. 7), and it correlated positively with body weights (wild type, r = 0.04, P = NS; OE-NPY$^{D\beta H}$, r = 0.64, $P < 0.05$). A strong correlation between glucose AUC and ghrelin was also observed in both genotypes (wild type, r = 0.57, $P < 0.05$; OE-NPY$^{D\beta H}$, r = 0.63, $P <$ 0.05).

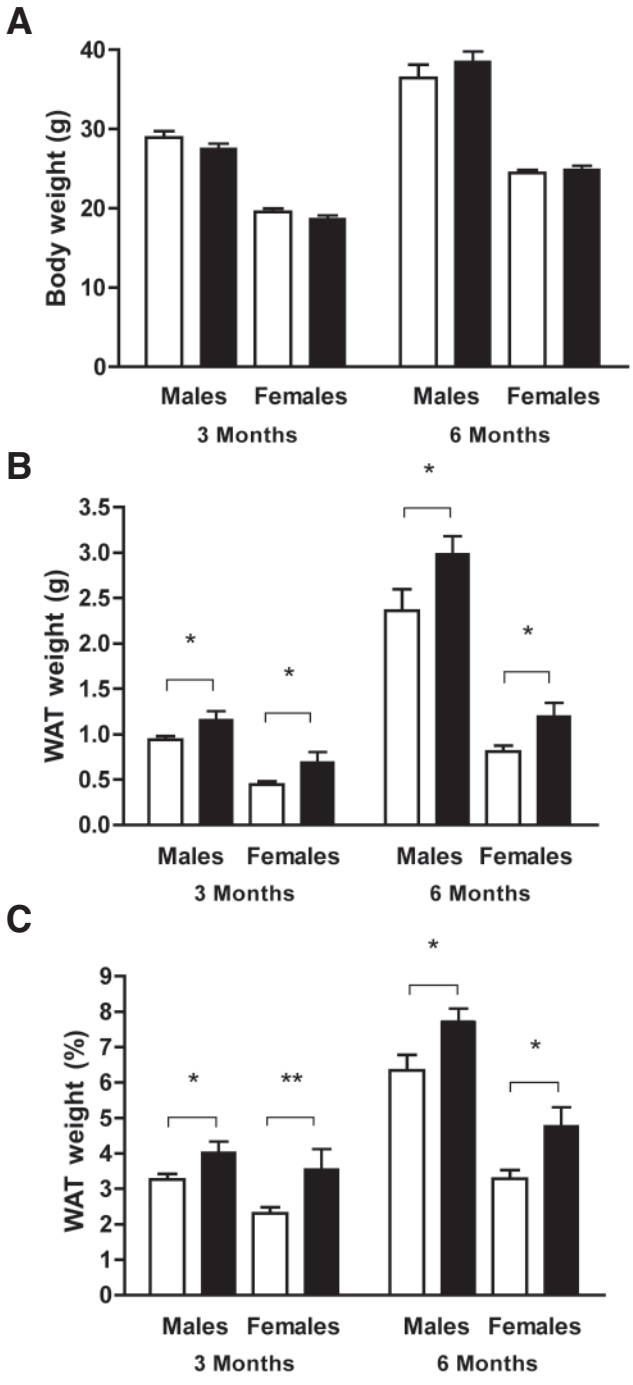

FIG. 4. Body weights and WAT weights. Mean body weights (*A*), WAT weights (*B*), and WAT per body weight (*C*) in percentages from male and female mice at 3 and 6 months of age (n = 8–15/group). Values are expressed as means ± SEM. □, wild-type mice; ■, OE-NPY$^{D\beta H}$ mice. *$P < 0.05$ and **$P < 0.01$ by Student's t test.

DISCUSSION

In this novel mouse model, we show that overexpression of NPY in noradrenergic neurons of the central and peripheral nervous systems leads to increased WAT mass and triglyceride accumulation in the liver already at an early age, leading to hyperinsulinemia and impaired glucose tolerance later in life. These changes occur without hyperphagia, increased body weight, hypercorticosteronemia, decreased BMD, or changes in locomotor activity or core temperature. Transgene expression is driven by the human DβH promoter, which has been used to generate transgenic mice in several other studies, and is shown to drive the transgene expression to noradrenergic neurons with very little ectopic expression (12,18,19). IRES sequence and *LacZ* reporter gene were inserted downstream of *preproNPY*, enabling the use of β-galactosidase staining as a marker of transgene expression. Because transgenic *preproNPY-IRES-LacZ* gene construct is transcribed to a single mRNA, detection of *LacZ* expression proves that *preproNPY* mRNA is also expressed in the same cells. β-Galactosidase staining showed that the transgene is strongly expressed in adrenal medulla and the locus coeruleus of the brainstem and faintly expressed in the hypothalamus, the thalamus, and the cortex, which fits

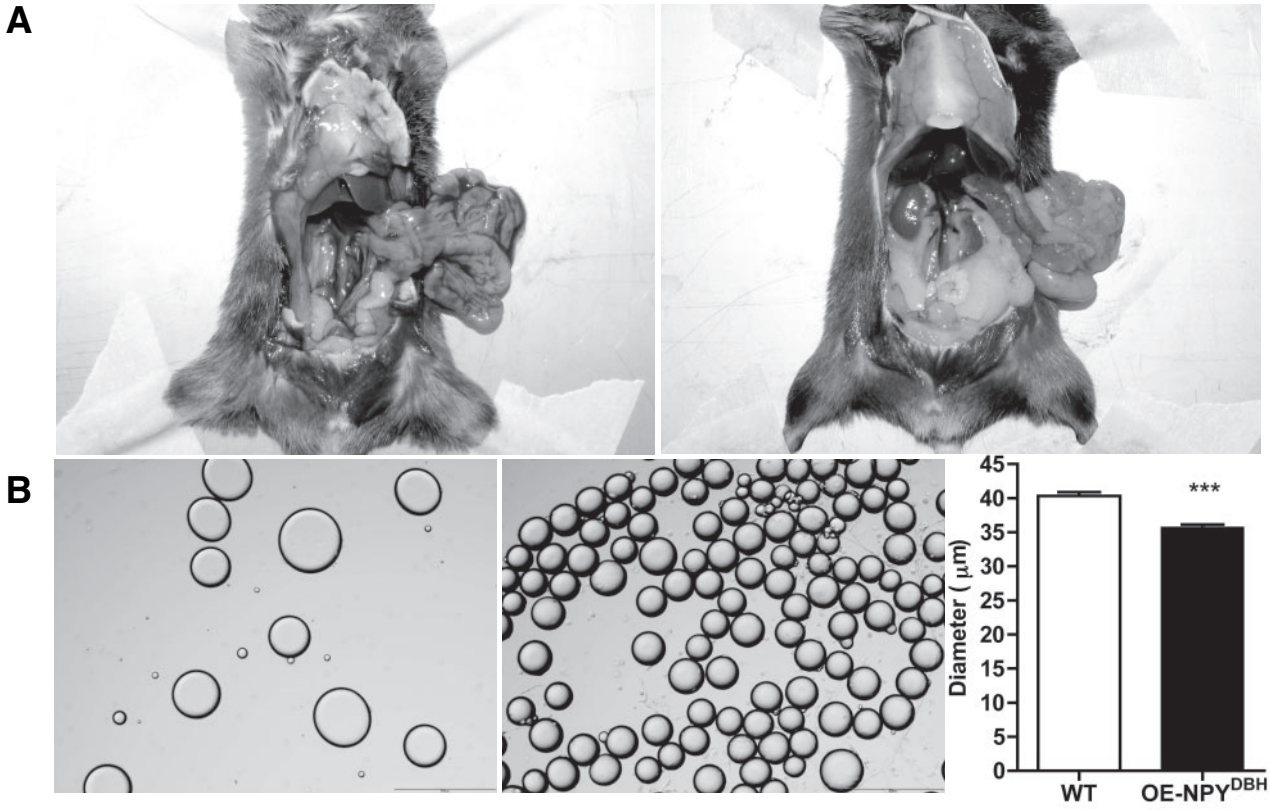

FIG. 5. Body fat composition and fat cell size. *A*: Three-month-old weight-matched mice: wild-type (*left*) and OE-NPY$^{D\beta H}$ (*right*) mice showing the amount of visceral WAT. *B*: Isolated fat cells from gonadal fat pads. Cells were isolated from wild-type (*left*) and OE-NPY$^{D\beta H}$ (*middle*) fat pads. Scale bar = 100 μm. The mean cell diameter in fat cells is presented in the *right panel* (wild type, n = 314 cells; OE-NPY$^{D\beta H}$, n = 565 cells). Values are expressed as means ± SEM. ***P < 0.001 by Mann-Whitney test.

with the previously described DβH expression pattern (12). NPY protein detection in tissue homogenates showed 1.3-fold increase in NPY in the adrenal glands and 1.8-fold in the brainstem dissection, including locus coeruleus and A5 noradrenergic nuclei, whereas there was no difference in the medial basal hypothalamus NPY in the OE-NPY$^{D\beta H}$ compared with wild-type mice. These data confirm that transgenic *preproNPY* mRNA is expressed in noradrenergic neurons and that total NPY peptide level is increased in areas of noradrenergic innervation.

The OE-NPY$^{D\beta H}$ mice have 20–25% increased body WAT depot mass compared with wild-type controls, which is observed already at the age of 3 months in both sexes. Fat cells from the transgenic mice are significantly smaller and, due to the heavier WAT weight, probably more numerous (hyperplasia). The finding is interesting because NPY has previously been linked to fat-cell hypertrophy, as central NPY administration promotes lipogenesis by stimulating lipoprotein lipase activity in WAT (5,20). In addition to increased WAT mass, triglyceride content in the liver is increased in 3- and 6-month-old OE-NPY$^{D\beta H}$ mice. Central administration of NPY or its Y5 receptor agonist have been shown to increase circulating levels of triglycerides (3,21), and chronic intracerebroventricular administration of NPY has been shown to stimulate de novo lipogenesis in the liver by increasing the hepatic acetyl CoA carboxylase activity (3). Hepatic steatosis in OE-NPY$^{D\beta H}$ mice could be a result of enhanced hepatic lipogenesis, or it may be secondary to increased fatty acid flux from the enlarged adipose tissue. In contrast, triglyc-

TABLE 1
Metabolic and endocrinological parameters

Variables measured	3 months			6 months		
	Wild type	OE-NPY$^{D\beta H}$	P value	Wild type	OE-NPY$^{D\beta H}$	P value
Liver triglyceride (mg/g tissue)	2.092 ± 0.093	2.415 ± 0.118	0.04	2.213 ± 0.170	2.992 ± 0.192	0.007
Triglyceride (mg/ml)	0.457 ± 0.057	0.472 ± 0.029	0.83	0.911 ± 0.089	1.046 ± 0.073	0.25
Cholesterol (μg/μl)*	ND	ND	—	1.593 ± 0.137	1.764 ± 0.082	0.33
Fasting insulin (μg/l)	<0.025†	<0.025†	—	1.596 ± 0.362	3.147 ± 0.605	0.04
Leptin (pg/ml)	645.7 ± 126.0	967.7 ± 158.5	0.17	5,596 ± 934.9	8,122 ± 896.9	0.06
Resistin (pg/ml)	1012 ± 130.1	722.4 ± 84.3	0.07	2,163 ± 133.2	2,186 ± 193.9	0.92
Corticosterone (ng/ml)	30.3 ± 4.2	42.3 ± 8.8	0.46	98.8 ± 32.9	78.4 ± 14.9	0.79
Ghrelin (pg/ml)	ND	ND	—	271.2 ± 82.0	368.8 ± 57.7	0.03

Data are means ± SEM, (n = 7–15/group). P value from Student's t test or Mann-Whitney test. Plasma (at 3 months) and serum (at 6 months) were used except for insulin, where plasma was used at all times. ND, not determined. *Measured from females. †The detection limit in Mercodia Ultrasensitive Mouse Insulin ELISA kit was 0.025 μg/l.

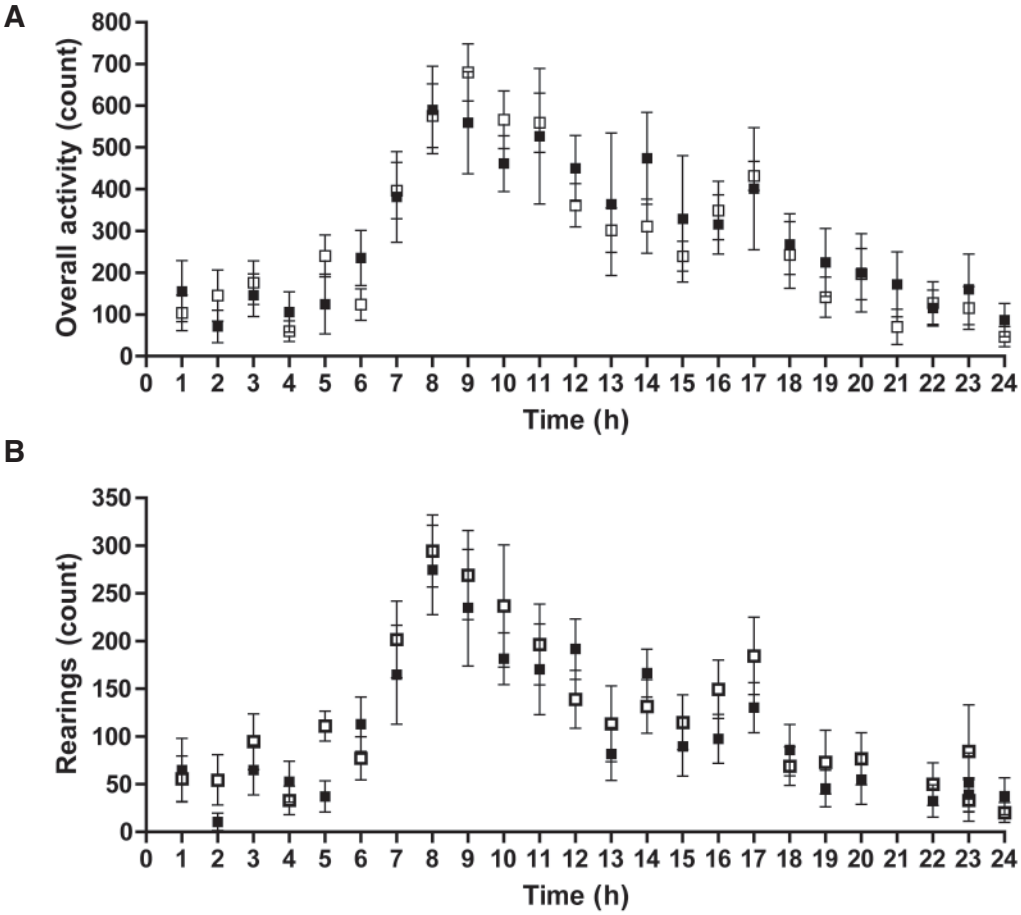

FIG. 6. Spontaneous locomotor activity test. Spontaneous 24-h locomotor activity (*A*) and number of rearings (*B*) from 5-month-old male mice (n = 8–11) were measured after an adjustment period to a novel environment. Values are expressed as means ± SEM. □, wild type mice; ■, OE-NPY$^{D\beta H}$ mice.

eride accumulation in the liver is not due to hyperinsulinemia, which has been shown to induce steatosis (22), because 3-month-old mice are not hyperinsulinemic but show hepatic steatosis.

OE-NPY$^{D\beta H}$ male mice are normoinsulinemic and glucose tolerant at the age of 3 months, but by the age of 6 months, they develop hyperinsulinemia and impaired glucose tolerance. These data show that chronically increased SNS NPY does not induce insulin release or affect glucose tolerance per se but augments hyperinsulinemia and impaired glucose tolerance associated with increased age and body weight. In contrast to male transgenic mice, glucose tolerance remains normal in 6-month-old females. The male and female mice differ in the degree of fat accumulation over age. Mean WAT weight (corrected with body weight) in 6-month-old males is twofold higher than in 3-month-old males compared with 1.4-fold increase in females both in wild-type and OE-NPY$^{D\beta H}$ mice (Fig. 4*C*). The sex difference in impairment of glucose tolerance may arise from the difference in development of excess adiposity. Thus, increased adiposity and liver triglyceride content seem to be the primary effects of NPY overexpression, and impaired glucose metabolism arises as an interaction between augmented fat accumulation and excess NPY in the OE-NPY$^{D\beta H}$ mice.

Serum ghrelin was significantly increased in the OE-NPY$^{D\beta H}$ mice over wild-type controls. Ghrelin is a gastric hormone associated with increased food intake and obesity. Central administration of ghrelin increases food intake, body weight, and adiposity (23–27), and this effect is mediated via stimulation of NPYergic neurons in the hypothalamus (24). In contrast, mouse models of

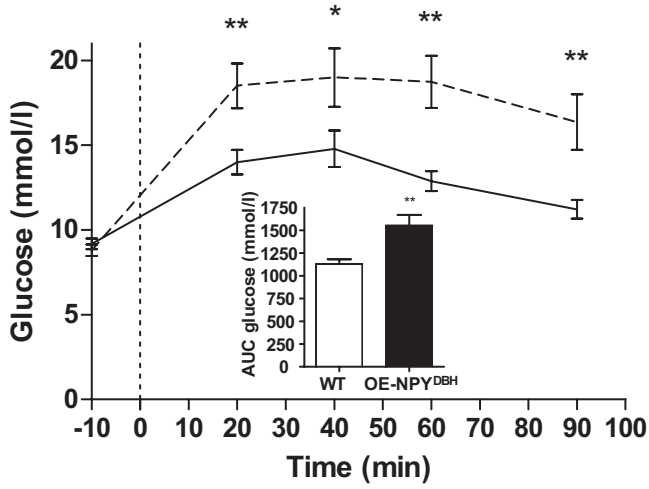

FIG. 7. IGTT of the 6-month-old male mice (n = 12–15) showing the mean blood glucose values at each time point (baseline, 20, 40, 60, and 90 min) of the test and the AUC in IGTT. The administration of glucose is marked at 0 min. Values are expressed as means ± SEM. Solid line and □, wild-type (WT) mice; hatched line and ■, OE-NPY$^{D\beta H}$ mice. *P < 0.05 and **P < 0.01 by repeated measures two-way ANOVA.

hyperghrelinemia have failed to show hyperphagia or obesity (28,29). These results fit with the phenotype of our OE-NPY$^{D\beta H}$ mice, i.e., hyperghrelinemia without hyperphagia. Furthermore, ghrelin has been implicated in the control of glucose metabolism. Acutely, ghrelin attenuates glucose-stimulated insulin release (30), and genetic ablation of ghrelin augments insulin release and stimulates glucose clearance after glucose injection (31). In our study, serum ghrelin strongly correlates with glucose AUC in IGTT, suggesting that increased circulating ghrelin contributes to impaired glucose tolerance in the OE-NPY$^{D\beta H}$ mice.

Increased adiposity in NPY-overexpressing mice is in line with previous studies in rats with chronic central infusion of NPY and Y2 receptor (Y2R)-null mice. In contrast to OE-NPY$^{D\beta H}$ mice, weight gain in these models is mainly due to hypothalamically mediated increase in food intake and decrease in energy expenditure (1,3,32). The effects of extrahypothalamic NPY on energy homeostasis have been scarcely addressed (33) until a recent paper by Kuo et al. (34), which shows stimulated NPY release from SNS by chronic mild stress to increase diet-induced obesity in mice. The effects of stress-induced NPY release on energy homeostasis fit the phenotype of the OE-NPY$^{D\beta H}$ mouse. The primary finding is increased WAT mass without change in food intake or body weight after 2 weeks of daily stress and high-fat diet. Prolonged stress and diet lead to liver steatosis, impaired glucose tolerance, and obesity, which are attenuated by local Y2R antagonist administration and fat-targeted *Y2*-gene knockdown procedure. Thus, SNS NPY seems to increase adipose tissue mass through local, Y2R-mediated mechanisms. Kuo et al. (34) show that NPY directly stimulates adipogenesis, i.e., proliferation and differentiation of preadipocytes in vitro, which correlates with the hyperplastic adipose tissue in our OE-NPY$^{D\beta H}$ model. Therefore, the phenotype of the OE-NPY$^{D\beta H}$ mouse closely resembles the effects of stress-induced NPY release from SNS on energy homeostasis, which supports that the phenotype is caused by overexpression of NPY in noradrenergic neurons.

In humans, association studies of a polymorphism in the *NPY* gene have linked NPY to metabolic disturbances. The L7P polymorphism, first described by our group, is associated with earlier onset of type 2 diabetes in obese carriers of L7P (35) and with other traits of the metabolic syndrome (36–39). Clinical studies have also shown that L7P carriers have altered insulin and ghrelin responses (40,41). L7P polymorphism is located in the signal peptide of the human *NPY* gene (36) and is functional leading to increased plasma levels of NPY during sympathetic activation in subjects carrying L7P allele (42). Thus, we have hypothesized that increased NPY causes the metabolic changes in L7P carriers. This hypothesis is now supported by the findings in OE-NPY$^{D\beta H}$ mice showing that even a modest chronic excess of NPY can lead to significant alterations in lipid and glucose metabolism.

In conclusion, moderate overexpression of NPY in SNS and brain noradrenergic neurons causes increased adiposity and liver triglyceride accumulation, which leads to hyperinsulinemia and impaired glucose tolerance with age. The effect seems to be nonhypothalamic because no difference is seen in the hypothalamic NPY content between the OE-NPY$^{D\beta H}$ mice and wild-type controls or in feeding and other hypothalamically induced NPY effects. These findings suggest that NPY exerts significant metabolic effects directly on peripheral target tissues and/or by modulation of autonomic nervous system activity. Furthermore, the results suggest that NPY may play an important role in the pathogenesis of disturbances in glucose and lipid metabolism. Thus, further analysis of the OE-NPY$^{D\beta H}$ mouse may provide an important tool for studies concerning the development of metabolic disorders and the role of NPY in the process.

ACKNOWLEDGMENTS

This study was supported by the Academy of Finland, the Finnish Funding Agency for Technology and Innovation, the Turku University Foundation, and the Finnish Cultural Foundation.

We thank Dr. Richard D. Palmiter (University of Washington) for providing the DβH promoter. Dr. Matti Poutanen and his staff (Transgenic Core Unit, University of Turku) are acknowledged for the microinjections. We thank Raija Kaartosalmi, Pipsa Lappalainen, Pirkko Huuskonen, Francisco Lopez-Picon, and Heikki Hiekkanen for technical and scientific assistance.

REFERENCES

1. Stanley BG, Kyrkouli SE, Lampert S, Leibowitz SF: Neuropeptide Y chronically injected into the hypothalamus: a powerful neurochemical inducer of hyperphagia and obesity. *Peptides* 7:1189–1192, 1986
2. Vettor R, Zarjevski N, Cusin I, Rohner-Jeanrenaud F, Jeanrenaud B: Induction and reversibility of an obesity syndrome by intracerebroventricular neuropeptide Y administration to normal rats. *Diabetologia* 37:1202–1208, 1994
3. Zarjevski N, Cusin I, Vettor R, Rohner-Jeanrenaud F, Jeanrenaud B: Chronic intracerebroventricular neuropeptide-Y administration to normal rats mimics hormonal and metabolic changes of obesity. *Endocrinology* 133:1753–1758, 1993
4. Dunbar JC, Ergene E, Barraco RA: Neuropeptide-Y stimulation of insulin secretion is mediated via the nucleus tractus solitarius. *Horm Metab Res* 24:103–105, 1992
5. Billington CJ, Briggs JE, Grace M, Levine AS: Effects of intracerebroventricular injection of neuropeptide Y on energy metabolism. *Am J Physiol* 260:R321–R327, 1991
6. Sainsbury A, Rohner-Jeanrenaud F, Cusin I, Zakrzewska KE, Halban PA, Gaillard RC, Jeanrenaud B: Chronic central neuropeptide Y infusion in normal rats: status of the hypothalamo-pituitary-adrenal axis, and vagal mediation of hyperinsulinaemia. *Diabetologia* 40:1269–1277, 1997
7. Erickson JC, Hollopeter G, Palmiter RD: Attenuation of the obesity syndrome of ob/ob mice by the loss of neuropeptide Y. *Science* 274:1704–1707, 1996
8. Pesonen U: Human NPY gene variants in cardiovascular and metabolic diseases. *Exs* 247–267, 2006
9. Gulbenkian S, Wharton J, Hacker GW, Varndell IM, Bloom SR, Polak JM: Co-localization of neuropeptide tyrosine (NPY) and its C-terminal flanking peptide (C-PON). *Peptides* 6:1237–1243, 1985
10. Ekblad E, Edvinsson L, Wahlestedt C, Uddman R, Hakanson R, Sundler F: Neuropeptide Y co-exists and co-operates with noradrenaline in perivascular nerve fibers. *Regul Pept* 8:225–235, 1984
11. Colmers WF, Bleakman D: Effects of neuropeptide Y on the electrical properties of neurons. *Trends Neurosci* 17:373–379, 1994
12. Mercer EH, Hoyle GW, Kapur RP, Brinster RL, Palmiter RD: The dopamine beta-hydroxylase gene promoter directs expression of *E. coli* lacZ to sympathetic and other neurons in adult transgenic mice. *Neuron* 7:703–716, 1991
13. Mountford PS, Smith AG: Internal ribosome entry sites and dicistronic RNAs in mammalian transgenesis. *Trends Genet* 11:179–184, 1995
14. Harvey NL, Srinivasan RS, Dillard ME, Johnson NC, Witte MH, Boyd K, Sleeman MW, Oliver G: Lymphatic vascular defects promoted by Prox1 haploinsufficiency cause adult-onset obesity. *Nat Genet* 37:1072–1081, 2005
15. Allen JM, Adrian TE, Polak JM, Bloom SR: Neuropeptide Y (NPY) in the adrenal gland. *J Auton Nerv Syst* 9:559–563, 1983
16. Di Girolamo M, Mendlinger S, Fertig JW: A simple method to determine fat cell size and number in four mammalian species. *Am J Physiol* 221:850–858, 1971
17. Folch J, Lees M, Sloane Stanley GH: A simple method for the isolation and

purification of total lipides from animal tissues. *J Biol Chem* 226:497–509, 1957
18. Kobayashi K, Sasaoka T, Morita S, Nagatsu I, Iguchi A, Kurosawa Y, Fujita K, Nomura T, Kimura M, Katsuki M, Nagatsu T: Genetic alteration of catecholamine specificity in transgenic mice. *Proc Natl Acad Sci U S A* 89:1631–1635, 1992
19. Kobayashi K, Morita S, Mizuguchi T, Sawada H, Yamada K, Nagatsu I, Fujita K, Nagatsu T: Functional and high level expression of human dopamine beta-hydroxylase in transgenic mice. *J Biol Chem* 269:29725–29731, 1994
20. Billington CJ, Briggs JE, Harker S, Grace M, Levine AS: Neuropeptide Y in hypothalamic paraventricular nucleus: a center coordinating energy metabolism. *Am J Physiol* 266:R1765–R1770, 1994
21. Mashiko S, Ishihara A, Iwaasa H, Sano H, Oda Z, Ito J, Yumoto M, Okawa M, Suzuki J, Fukuroda T, Jitsuoka M, Morin NR, MacNeil DJ, Van der Ploeg LH, Ihara M, Fukami T, Kanatani A: Characterization of neuropeptide Y (NPY) Y5 receptor-mediated obesity in mice: chronic intracerebroventricular infusion of D-Trp(34)NPY. *Endocrinology* 144:1793–1801, 2003
22. Qureshi K, Abrams GA: Metabolic liver disease of obesity and role of adipose tissue in the pathogenesis of nonalcoholic fatty liver disease. *World J Gastroenterol* 13:3540–3553, 2007
23. Asakawa A, Inui A, Kaga T, Katsuura G, Fujimiya M, Fujino MA, Kasuga M: Antagonism of ghrelin receptor reduces food intake and body weight gain in mice. *Gut* 52:947–952, 2003
24. Asakawa A, Inui A, Kaga T, Yuzuriha H, Nagata T, Ueno N, Makino S, Fujimiya M, Niijima A, Fujino MA, Kasuga M: Ghrelin is an appetite-stimulatory signal from stomach with structural resemblance to motilin. *Gastroenterology* 120:337–345, 2001
25. Faulconbridge LF, Cummings DE, Kaplan JM, Grill HJ: Hyperphagic effects of brainstem ghrelin administration. *Diabetes* 52:2260–2265, 2003
26. Theander-Carrillo C, Wiedmer P, Cettour-Rose P, Nogueiras R, Perez-Tilve D, Pfluger P, Castaneda TR, Muzzin P, Schurmann A, Szanto I, Tschop MH, Rohner-Jeanrenaud F: Ghrelin action in the brain controls adipocyte metabolism. *J Clin Invest* 116:1983–1993, 2006
27. Tschop M, Smiley DL, Heiman ML: Ghrelin induces adiposity in rodents. *Nature* 407:908–913, 2000
28. Wei W, Qi X, Reed J, Ceci J, Wang HQ, Wang G, Englander EW, Greeley GH Jr: Effect of chronic hyperghrelinemia on ingestive action of ghrelin. *Am J Physiol Regul Integr Comp Physiol* 290:R803–R808, 2006
29. Iwakura H, Hosoda K, Son C, Fujikura J, Tomita T, Noguchi M, Ariyasu H, Takaya K, Masuzaki H, Ogawa Y, Hayashi T, Inoue G, Akamizu T, Hosoda H, Kojima M, Itoh H, Toyokuni S, Kangawa K, Nakao K: Analysis of rat insulin II promoter-ghrelin transgenic mice and rat glucagon promoter-ghrelin transgenic mice. *J Biol Chem* 280:15247–15256, 2005
30. Dezaki K, Hosoda H, Kakei M, Hashiguchi S, Watanabe M, Kangawa K, Yada T: Endogenous ghrelin in pancreatic islets restricts insulin release by attenuating Ca^{2+} signaling in β-cells: implication in the glycemic control in rodents. *Diabetes* 53:3142–3151, 2004
31. Sun Y, Asnicar M, Saha PK, Chan L, Smith RG: Ablation of ghrelin improves the diabetic but not obese phenotype of ob/ob mice. *Cell Metab* 3:379–386, 2006
32. Naveilhan P, Hassani H, Canals JM, Ekstrand AJ, Larefalk A, Chhajlani V, Arenas E, Gedda K, Svensson L, Thoren P, Ernfors P: Normal feeding behavior, body weight and leptin response require the neuropeptide Y Y2 receptor. *Nat Med* 5:1188–1193, 1999
33. Vettor R, Pagano C, Granzotto M, Englaro P, Angeli P, Blum WF, Federspil G, Rohner-Jeanrenaud F, Jeanrenaud B: Effects of intravenous neuropeptide Y on insulin secretion and insulin sensitivity in skeletal muscle in normal rats. *Diabetologia* 41:1361–1367, 1998
34. Kuo LE, Kitlinska JB, Tilan JU, Li L, Baker SB, Johnson MD, Lee EW, Burnett MS, Fricke ST, Kvetnansky R, Herzog H, Zukowska Z: Neuropeptide Y acts directly in the periphery on fat tissue and mediates stress-induced obesity and metabolic syndrome. *Nat Med* 13:803–811, 2007
35. Jaakkola U, Pesonen U, Vainio-Jylha E, Koulu M, Pollonen M, Kallio J: The Leu7Pro polymorphism of neuropeptide Y is associated with younger age of onset of type 2 diabetes mellitus and increased risk for nephropathy in subjects with diabetic retinopathy. *Exp Clin Endocrinol Diabetes* 114:147–152, 2006
36. Karvonen MK, Pesonen U, Koulu M, Niskanen L, Laakso M, Rissanen A, Dekker JM, Hart LM, Valve R, Uusitupa MI: Association of a leucine(7)-to-proline(7) polymorphism in the signal peptide of neuropeptide Y with high serum cholesterol and LDL cholesterol levels. *Nat Med* 4:1434–1437, 1998
37. Niskanen L, Karvonen MK, Valve R, Koulu M, Pesonen U, Mercuri M, Rauramaa R, Toyry J, Laakso M, Uusitupa MI: Leucine 7 to proline 7 polymorphism in the neuropeptide Y gene is associated with enhanced carotid atherosclerosis in elderly patients with type 2 diabetes and control subjects. *J Clin Endocrinol Metab* 85:2266–2269, 2000
38. Karvonen MK, Valkonen VP: Leucine7 to proline7 polymorphism in the preproneuropeptide Y is associated with the progression of carotid atherosclerosis, blood pressure and serum lipids in Finnish men. *Atherosclerosis* 159:145–151, 2001
39. Niskanen L, Voutilainen-Kaunisto R: Leucine 7 to proline 7 polymorphism in the neuropeptide y gene is associated with retinopathy in type 2 diabetes. *Exp Clin Endocrinol Diabetes* 108:235–236, 2000
40. Jaakkola U, Kuusela T, Jartti T, Pesonen U, Koulu M, Vahlberg T, Kallio J: The Leu7Pro polymorphism of preproNPY is associated with decreased insulin secretion, delayed ghrelin suppression, and increased cardiovascular responsiveness to norepinephrine during oral glucose tolerance test. *J Clin Endocrinol Metab* 90:3646–3652, 2005
41. Kallio J, Pesonen U, Karvonen MK, Kojima M, Hosoda H, Kangawa K, Koulu M: Enhanced exercise-induced GH secretion in subjects with Pro7 substitution in the prepro-NPY. *J Clin Endocrinol Metab* 86:5348–5352, 2001
42. Kallio J, Pesonen U, Kaipio K, Karvonen MK, Jaakkola U, Heinonen OJ, Uusitupa MI, Koulu M: Altered intracellular processing and release of neuropeptide Y due to leucine 7 to proline 7 polymorphism in the signal peptide of preproneuropeptide Y in humans. *FASEB J* 15:1242–1244, 2001